PLUTO–CHARON STELLAR OCCULTATION CANDIDATES: 1990–1995

E. W. DUNHAM
NASA Ames Research Center, Moffett Field, California 94035

S. W. MCDONALD
Department of Earth, Atmospheric, and Planetary Sciences, Massachusetts Institute of Technology, Cambridge, Massachusetts 02139

J. L. ELLIOT
Department of Earth, Atmospheric, and Planetary Sciences, Massachusetts Institute of Technology, Cambridge, Massachusetts 02139
and
Department of Physics, Massachusetts Institute of Technology, Cambridge, Massachusetts 02139
Received 1 May 1991; revised 14 June 1991

ABSTRACT

We have carried out a search to identify stars that might be occulted by Pluto or Charon during the period 1990–1995 and part of 1996. This search was made with an unfiltered CCD camera operated in the strip scanning mode, and it reaches an R magnitude of approximately 17.5—about 1.5 mag fainter than previous searches. Circumstances for each of the 162 potential occultations are given, including an approximate R magnitude of the star, which allows estimation of the signal-to-noise ratio (S/N) for observation of each occultation. The faintest stars in our list would yield an S/N of about 20 for a 1 s integration when observed with a CCD detector on an 8 m telescope under a dark sky. Our astrometric precision (± 0.2 arcsec, with larger systematic errors possible for individual cases) is insufficient to serve as a final prediction for these potential occultations, but is sufficient to identify stars deserving of further, more accurate, astrometric observations. Statistically, we expect about 32 of these events to be observable somewhere on Earth. The number of events actually observed will be substantially smaller because of clouds and the sparse distribution of large telescopes. Finder charts for each of the 91 stars involved are presented.

1. INTRODUCTION

There has been an enormous increase in observational data on, and theoretical interest in, the Pluto–Charon system in recent years (see, for example, Binzel 1989 and other articles in the same issue). This is partly due to the recent series of mutual eclipses and occultations in the system (see, for example, Binzel *et al.* 1985; Tholen & Buie 1989), and partly to the observation of the 1988 stellar occultation of P8 by Pluto (e.g., Elliot *et al.* 1989). Stellar occultations provide by far the highest spatial resolution observations of the system and the only means of directly probing Pluto's atmosphere. Outstanding questions that can be answered by further occultation observations are: (i) how does the structure of Pluto's atmosphere change with season, and (ii) does a haze layer exist in Pluto's lower atmosphere? Also, further stellar occultation data can contribute to the analysis of the mutual event data by providing the radii of the visible disks of Pluto and Charon, and constraints on the semimajor axis of the system (if an occultation of the same star by both Pluto and Charon can be observed). The issue of whether Charon has an atmosphere remains an open question. Elliot & Young (1991) recently reanalyzed the data from the 1980 stellar occultation by Charon (Walker 1980) and found tantalizing, but inconclusive, evidence that Charon has a very tenuous atmosphere. Since the Pluto–Charon system has recently passed perihelion, Pluto's atmosphere will be reacting to the reduction in sunlight, and if Charon has a detectable atmosphere, it will be most noticeable during the next decade or two.

A recent paper by Mink *et al.* (1991, hereafter referred to as MKB) has presented the results of a photographic search for Pluto and Charon occultation candidates that reached a V magnitude of approximately 16. However, even the faintest stars in their list would result in observations with an S/N ratio of 30 if observed with a 4 m telescope and a sensitive detector, so many useful occultation candidates fainter than their magnitude limit were missed. Therefore, we have carried out a program to identify fainter stars which might be occulted by either Pluto or Charon over the period from 1990 to 1995.

The method used here is CCD strip scanning—similar to that described by Gehrels *et al.* (1986) and Benedict *et al.* (1991). The columns of the CCD are oriented along the E–W direction in the telescope's focal plane, the telescope is left stationary, and the rows of the CCD are clocked out at the same rate that the star images drift across the CCD. The resulting images, or strips, are as wide as the CCD in declination (Dec.), but are as long as desired in right ascension (R.A.). Stellar images on the strips are then identified and an astrometric solution is carried out to allow assignment of celestial coordinates to each identified star. The ephemerides of Pluto and Charon are then compared with the lists of stars, and all stars within some threshold distance of the ephemeris are identified. Thus, our procedure is essentially the same as classical photographic astrometry with the exception that the images are obtained with a CCD. Nevertheless, there are enough differences that we shall discuss our observed astrometric precision and accuracy in considerable detail.

An additional benefit of making the observations with a CCD is that the CCD magnitudes are more reliable than photographic magnitudes, as proved to be the case for P8 (Bosh *et al.* 1986). We did not attempt to make accurate photometric calibrations when making the observations, but during the analysis of our data we found that it was possible

 0004-6256/91/041464-21$00.90

to obtain reasonably reliable magnitudes by using as standards those stars for which photoelectric magnitudes were presented in MKB.

It should be emphasized that the accuracy of the positions given here is only sufficient to serve as a means of filtering out events that have a chance of being visible somewhere on the Earth, not to serve as input for producing believable occultation ground tracks.

2. INSTRUMENTATION AND OBSERVATIONS

The observations were made with CCD 1 of the SNAPSHOT CCD camera (Dunham *et al.* 1985) operated in a scanning mode, as described above. A significant recent change made in the camera was the replacement of the 12-bit A/D converter and programmable gain amplifier with the 16-bit A/D converter circuit described by Luppino (1989). The system's dynamic range was limited to about 14 bits by the CCD itself rather than the A/D converter. Tests of photometric linearity showed a 2% error at 10 000 ADU's increasing rapidly with signal level and ultimately saturating at about 22 000 ADU's.

The CCD temperature was regulated to ensure that subtraction of dark current and field flattening would be effective. While we were setting up the flattening procedure before beginning the observing run, we discovered that the charge transfer efficiency (CTE) of CCD 1 was very poor at the very low signal levels found in dark frames. The poor CTE washed out the structure in the dark frame that needed to be removed, mainly electrical bias structure and a stripe down the center of the strip due to a single hot pixel near the center of the chip. We worked around this problem by taking dark strips with the shutter open and the dome closed with the lights off. This introduced a small background level and restored the normal CTE. Flatfield strips were taken with the telescope pointed at a white surface in the dome illuminated diffusely by a quartz halogen lamp, after reflecting from two flat white surfaces. The flat strips have no structure as a function of row number because each image is an average exposure over all the rows, but the illumination falls off somewhat toward the edges in the column direction. The nonuniformity of the flat field has no effect on finding stars or on determining their position because these operations are done relative to the local background level, but it does affect the photometry at the 0.1 mag level.

The camera was mounted at the Cassegrain focus of the 0.61 m telescope at MIT's Wallace Astrophysical Observatory, in Westford, Massachusetts. The stellar images initially had a FWHM of 5–6 arcsec, but we were able to reduce the FWHM to about 4.5 arcsec under most circumstances by installing large fans to draw air in through the dome's slot and also in through the telescope tube. This had the effect of suppressing the irregular turbulence produced by convective cooling of the telescope and interior structures in the dome. We installed reducing optics in the camera to produce an image scale of 2.28 arcsec/pixel. This was close to the best compromise between fully sampling a seeing disk and getting the widest strip possible. These highly successful reducing optics were made using stock catalog lenses with optimized spacings determined for us by Greg Aldering, and are described in detail by Williams (1988). A similar system is described by Aldering (1990). This image scale resulted in strips about 15 arcmin wide in declination and an effective exposure time of approximately 90 s.

We chose to lay out the strips with nearly 50% overlap so that almost all stars would be found twice. The two exposures provided a check on the reality of an image and a means for making an external estimate of the astrometric and photometric precision. In addition, the large strip overlap made it possible to carry out the photometric "bootstrapping" process described below. Some of the strips were reobserved because of high background levels or other adverse circumstances. The log of the observations appears in Table 1. We obtained enough strips to completely cover the path of Pluto's ephemeris from 1990 to 1995, and for most of 1996. Only the earliest and latest parts of 1996 (including the event P29; see Fig. 1) were not covered.

We chose to make the observations with no filter in order to maximize the depth of the search at the expense of incurring additional uncertainties due to refraction. We made our observations at altitudes above 30° as a compromise between minimizing refraction effects and maximizing the available observing time. The magnitude of refractive position errors as a function of star color is evaluated in Sec. 4. We were also concerned about the combined effects of differential refraction in declination and distortion introduced by the reducing optics. These were checked for by carrying out both quadratic and linear plate solutions.

We could not use the SAO or AGK3 catalog stars as astrometric standards because they are all too bright. Instead, we used the list of stars searched by MKB. The stars in this list are clustered around Pluto's ephemeris, and so are not distributed at all uniformly across the strips, as may be seen from Fig. 1. This distribution of astrometric standards is not ideal, but systematic position errors did not arise because the occultation candidates are surrounded by standards (see Sec. 4).

3. ANALYSIS PROCEDURES

3.1 Astrometry

We created a software "pipeline" to analyze the 7 Mbytes of data produced by each strip scan. The goal of the pipeline was to minimize the manual intervention required in the analysis to reduce the calendar time and manpower required for the analysis. We used release 2.8 of the IRAF package (Tody 1986) including the beta test version of DAOPHOT (Stetson 1987) as the core components of the pipeline. The steps in the pipeline carried out for each strip are described briefly below.

(1) Break each strip into three sections, each of a size manageable by IRAF on our computers.

(2) Flatten each section with IRAF, using the dark strips and flat-field strips. On each night, we took a series of low-light dark strips, some 200–300 ADU's above the true mean dark level. We also took some true zero-light dark strips. IRAF determined the mean levels of the zero-light dark images and the mean levels of the low-light dark images, and subtracted the difference from the low-light dark image to create an artificial dark image with the correct mean value. This dark image would have some flatfield characteristics, but at the level of the low-light dark, dark features dominate. From there we proceeded to flatten the images in fairly straightforward fashion, using the image, the flat, and the dark produced in the above procedure. In the equations below, the subscript i refers to the ith row and j to the jth column. D_j refers to the artificial dark strip, L_j the low-light dark strip, $\overline{Z}$ the average zero-light dark strip, R_{ij} the raw strip, I_{ij} the calibrated strip, and F_j the flat strip.

TABLE 1. Observations.

Strip Number	UT Date Taken (yy mm dd)	FWHM (")	Background above bias (ADU's)	Limiting Open CCD Magnitude	Comments
1	90 03 22	4.86	600	17.8	very poor astrometry
2	90 03 22	4.86	650	17.8	
3	90 03 22	4.86	800	17.8	
4	90 03 19	3.81	800	17.8	
5	90 03 28	4.22	1200	17.6	Incorrect clock rate
6	90 03 28	4.22	1100	18.0	Incorrect clock rate
7	90 03 28	4.22	975	18.1	Incorrect clock rate
8	90 03 28	4.22	850	18.1	
9	90 03 28	4.22	800	18.1	poor astrometry
10	90 03 28	4.22	775	18.2	
11	90 03 28	4.22	800	18.2	
12	90 03 29	4.79	975	18.2	
13	90 03 29	4.79	850	18.2	
14	90 03 29	4.79	775	18.2	
15	90 03 29	3.81	725	18.2	poor astrometry
16	90 03 29	3.81	700	18.0	poor astrometry
17	90 03 29	3.81	725	17.8	
18	90 04 13	4.63	2600-2750	17.6	
18A	90 06 13	4.17	900	17.6	
18B	90 06 18	4.08	1150	17.6	
19	90 04 13	4.63	2650-2800	17.6	
19A	90 06 18	4.08	1050	17.6	
20	90 04 13	4.63	2825	17.5	
20A	90 06 18	4.08	1050	17.5	
21	90 05 11	4.65	3125	17.8	
21A	90 06 26	3.69	700	17.8	
22	90 05 11	4.65	3300	17.7	
22A	90 06 26	3.69	700	17.7	
23	90 05 11	4.65	3400	17.7	
23A	90 06 26	3.69	700	17.7	
24	90 05 11	4.65	4200	---	moon too bright; not useable
24A	90 06 26	3.69	800	17.6	poor astrometry
25	90 05 14	4.35	950	17.7	
25A	90 06 26	3.69	850	17.7	poor astrometry, 25° altitude
26	90 05 14	4.35	1250	17.7 (V)	variable cirrus clouds
26A	90 06 27	---	900	17.7	
27	90 05 14	4.35	1650	17.6 (V)	variable cirrus clouds
27A	90 06 27	---	1500	16.4	poor astrometry; CCD warming
28	90 05 27	4.47	925	17.8	
28X	90 05 14	4.35	1900-2300 (V)	17.6 (V)	variable cirrus clouds
29	90 05 27	4.47	1025	17.7	
30	90 05 27	4.47	1400	17.7	poor astrometry
31	90 05 31	5.70	1050	17.6	
32	90 05 31	5.70	950	17.8	
33	90 05 31	5.70	650	17.2	
34	90 05 31	5.70	750	17.6	
35	90 05 31	5.70	725	17.6	
36	90 05 31	5.70	475	17.0	poor astrometry
37	90 05 31	5.70	800	17.4	
38	90 06 01	4.13	1325	17.6	
39	90 06 01	4.13	1200	17.6	
40	90 06 01	4.13	1100	17.6	
41	90 06 01	4.13	1050	17.6	
42	90 06 01	4.13	950	17.5	
43	90 06 01	4.13	800	17.3	
44	90 06 01	4.13	800	17.0	
45	90 06 01	4.13	850	17.0	poor astrometry
46	90 06 01	4.13	900	17.0	CCD warming; bad clock rate
47	90 06 02	5.02	1600	17.6	
48	90 06 02	5.02	1350-1650 (V)	17.6 (V)	spotty clouds
48A	90 06 13	4.17	925	17.6	
49	90 06 02	5.02	850-1900 (V)	17.5 (V)	poor astrometry, spotty clouds
49A	90 06 13	4.17	950	17.6	
50	90 06 02	5.02	1150-1300 (V)	17.5 (V)	spotty clouds
51	90 06 02	5.02	850	17.5	
52	90 06 02	5.02	800	17.4	

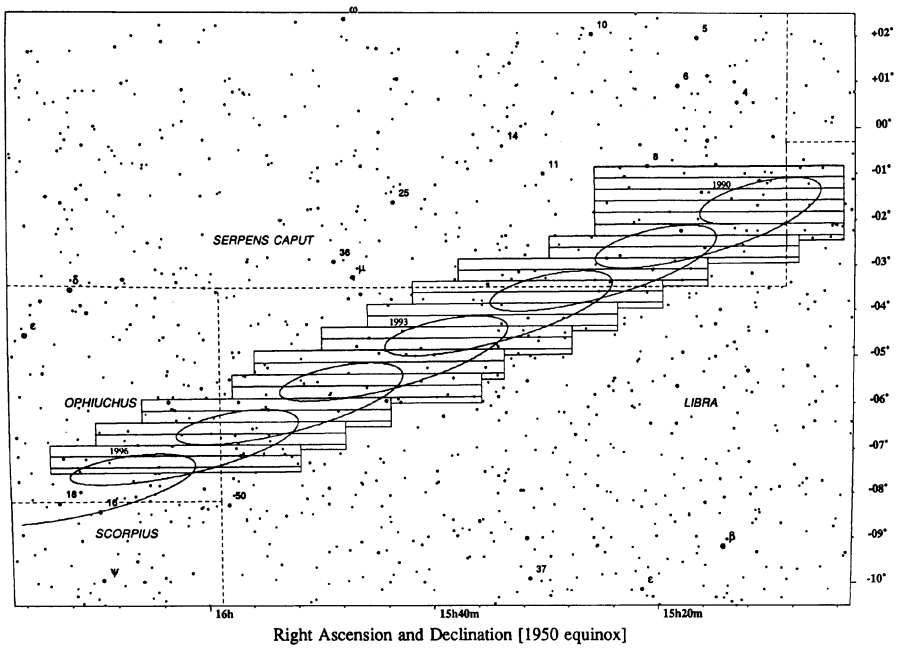

FIG. 1. Strip layout. The odd numbered strips are shown against a background of SAO catalog stars with Pluto's ephemeris superimposed. Our astrometric standard stars are clustered tightly around Pluto's ephemeris. The even numbered strips are centered on the edges of the adjacent odd numbered strips. Strip 1 is the northernmost strip. The ephemeris begins on 1 January 1990, on the boundary between strips 9 and 11. The 1996 retrograde loop is only partially covered.

$$D_j = L_j - (\overline{L} - \overline{Z}), \tag{1}$$

$$I_{ij} = \frac{(R_{ij} - D_j)\ \overline{(F_j - D_j)}}{(F_j - D_j)} + \overline{Z}. \tag{2}$$

This produced a flattened image with the same ADU scale and offset as the original image.

(3) Run the DAOPHOT procedures FIND, PHOT, PSF, GROUP, and NSTAR on each section. We ignored pixels with signals above 10 000 ADU's for purposes of point spread function fitting in order to avoid the nonlinear response of the CCD at high signal levels. Thus, stars with peak pixels higher than this threshold (about 12th mag) were still detected and fitted, but the pixels in a core area which were above the threshold were not included in the fit. If the star is particularly bright (about 9th mag), the image bleeds down the CCD columns, which damages both astrometry and photometry, but in general the wings of a bright-star image give reasonably accurate measurements for astrometry and photometry. The final product is a list of all stars detected automatically on each section, with position and photometry.

(4) Combine the results of each section to make a single list of star positions and magnitudes for each strip.

(5) Examine the strip with *ximage*, an *X*-window image display utility, to identify one or more stars with either stars on an overlapping strip or with stars in the MKB list.

(6) Match stars from the strip to the standard star list.

(7) Examine the list of matches; discard any that were fitted poorly by DAOPHOT. Stars showing poor fits were usually either very bright or close to the edge of the strip.

(8) Register the stars from the strip against the standard stars, producing the equivalent of a plate solution for the strip. We decided to use a linear rather than quadratic plate solution because the linear solution produced star positions that matched better between neighboring strips. One possible explanation for this is the fact that the standard star set we were using did not cover the entire field of each strip, but crossed it in bands. Either solution should be good in the neighborhood of the ephemeris, where the standard stars were distributed, but outside of that neighborhood the solutions are less reliable. The quadratic solution in particular could allow the solution away from the region of the standard stars to vary quite a bit, and neighboring strips thus could have a greater discrepancy in star positions with the quadratic solution. Another factor is that the standard stars we used were measured by MKB from several different photographic plates. The plate solutions derived for these plates did not mesh perfectly at the intersections between plates, and thus our standard stars may have had a systematic error dependent on where they appeared on MKB's original plates. A final consideration in our decision to use a linear plate solution is that a strip scan should inherently have a linear solution along the axis of right ascension. The plate solution along that axis is entirely determined by the clocking rate of the strip scan.

(9) Use the plate solution determined above to convert all the star positions from the strip into R.A. and Dec.

(10) Step through the ephemerides of Pluto and Charon to find all stars on the strip which are within a specified distance from each ephemeris. The ephemerides were provided to us at 1 day intervals by Doug Mink, and were de-

rived from the JPL DE-130 ephemeris (Standish 1987) assuming a Charon/Pluto mass ratio of 0.152.

Steps (1)–(4) were carried out with a shell script, which automatically ran the splitting and recombining procedures and called up an IRAF CL language script to perform the flattening and DAOPHOT routines. The CL script included an algorithm for selecting sufficiently well-profiled stars for determining the point spread function. Thus the entire process of locating stars on the CCD images was carried out automatically. The remainder of the steps were done separately so that we could evaluate the results at each stage.

As the strip analyses were completed, the candidate star list was updated, and matching events found on overlapping strips were identified. A new list of all the candidates was made, with mean positions for stars identified on two or more strips. Finally, this list was compared to the ephemeris again to find the occultation circumstances based on the mean star positions.

3.2 Photometry

Photometric calibration was performed separately. After all the strips were analyzed astrometrically, all stars which appeared on the overlapping region of two strips were identified. For each star found on the two strips, the instrumental magnitude as determined on the two strips was compared. The magnitude difference as found on the two strips was weighted by the signal, and this was summed over all the overlapping stars and divided by the sum of the weights. This produced an overall magnitude difference between the two given strips. The magnitude difference is caused by differing levels of extinction during the two strips. DAOPHOT typically found 2000–3000 stars on each strip, so generally over 1000 stars were compared between each pair of overlapping strips.

Given the difference between the instrumental magnitudes of each pair of overlapping strips and a photometric standard star on one of the strips, it is a simple matter to determine photometric magnitudes on that one strip and bootstrap to neighboring strips, continuing until all strips are reduced. MKB provided *UBVRI* and *K* magnitudes for several of the Pluto occultation candidates, and we used five of these candidates to photometrically reduce our strips. These five candidates were: P12, appearing on strips 2 and 3; P17 on strips 18, 18A, 18B, 19, and 19A; P20 on strips 33 and 34; P27 on strips 42 and 43; and P24 on strips 48, 48A, 49, and 49A. Our unfiltered CCD detector has already been determined to have a response similar to an *R* filter, so we used MKB's *R* magnitudes and consider our magnitudes to be close to Kron–Cousins *R* magnitudes. We divided our strips into five sets—each set was reduced by the above method using the photometric standard which appeared in the midst of that set. The dividing lines between the sets were largely determined by the existence of several strips which did not seem to work well with the bootstrapping method, probably due to varying extinction across a strip. In general the bootstrapping method seemed to work well, giving good agreement between strips, but there are exceptions introducing errors of several tenths of a magnitude on strips bootstrapped beyond them. Therefore our magnitudes for candidates should be treated as approximate.

A comparison of our magnitudes to the photographic (*V*) magnitudes of MKB is shown in Fig. 2. A clear trend can be seen in the figure, with the photographic magnitudes being about 0.5 mag fainter for the bright stars, and a similar amount brighter for the faint stars. The difference for the brighter stars is simply due to the different spectral responses; the average $V - R$ color of the seven stars measured by Buie and presented in MKB is $+0.44$. The trend for the fainter stars confirms MKB's suspicions that their magnitudes might be too bright for the fainter stars.

4. ASTROMETRY

4.1 Precision

We assessed the precision of our astrometry by examining the difference between the position of each star image and the mean position of that star as derived from all the images of that star. In most cases, there were two measured positions of a star from the two overlapping strips in which the star fell. Some strips were taken more than once so most stars on these strips have more than two observations. The results from our most heavily observed overlap region (the strip 18 and 19 overlap region, an otherwise typical case) are illustrative and are shown in Fig. 3. In this sample, each star was observed five times. The standard deviation of the distribution of position residuals about the mean is 0.11 arcsec in R.A. and 0.18 arcsec in Dec. Of course, the standard deviation increases with increasing stellar magnitude.

For faint stars, the expected precision is limited by the photon noise from the sky background. Following the analysis of Stier (1986), we find the uncertainty in either R.A. or Dec. in pixels to be given by

$$\sigma_x \cong \sigma W^2 / 4 S_{\rm tot}, \tag{3}$$

where σ is the rms uncertainty per pixel in the sky level, W is the FWHM of the point spread function in pixels, and $S_{\rm tot}$ is the total signal from the star. For our observed values of σ, W, and $S_{\rm tot}$, we expect a precision based on shot noise in the background of $\sigma_x = 0.01$ pixels (0.03 arcsec) for an $R = 17$ mag star. Clearly, other noise sources in our data are more important than this.

The comparison between some strips was much worse than the typical comparison, indicating particularly poor astrometry; these are noted in Table 1. A few strips actually seem to have two overlapping wedge patterns, possibly indicating that the telescope shifted during the observation. Further investigation revealed the presence of a pervasive low-frequency motion of the sky coordinate system relative to the CCD. Figure 4 shows the deviation of the five individual positions of each star in the strip 18 and 19 overlap region from the mean of the five positions of each star as a function of the R.A. of the star (or alternatively, the sidereal time). The residuals for each strip have been offset to make the low-frequency variations easier to see. Clearly, most of the variation is in Dec., with a peak-to-peak amplitude of about 0.3 arcsec. This instability could be caused by (1) a 3 μrad tilt of the telescope's secondary mirror due to wind loading, (2) a 0.3 arcsec pointing variation in the telescope due to wind loading, or (3) a 0.5% change in the density of the air along the line of sight, causing a change in the refraction angle. Since these strips were all taken at an hour angle of 17° or less, a change in refraction angle in the vertical direction would cause less than 1/4 as much R.A. offset as Dec. offset, so any R.A. variation would be unobservable in this dataset.

Observers at the U.S. Naval Observatory have noticed similar effects in their CCD strip-scanning data using a 20 cm telescope (R. Stone, private communication). Their position instability is almost certain to be atmospheric in na-

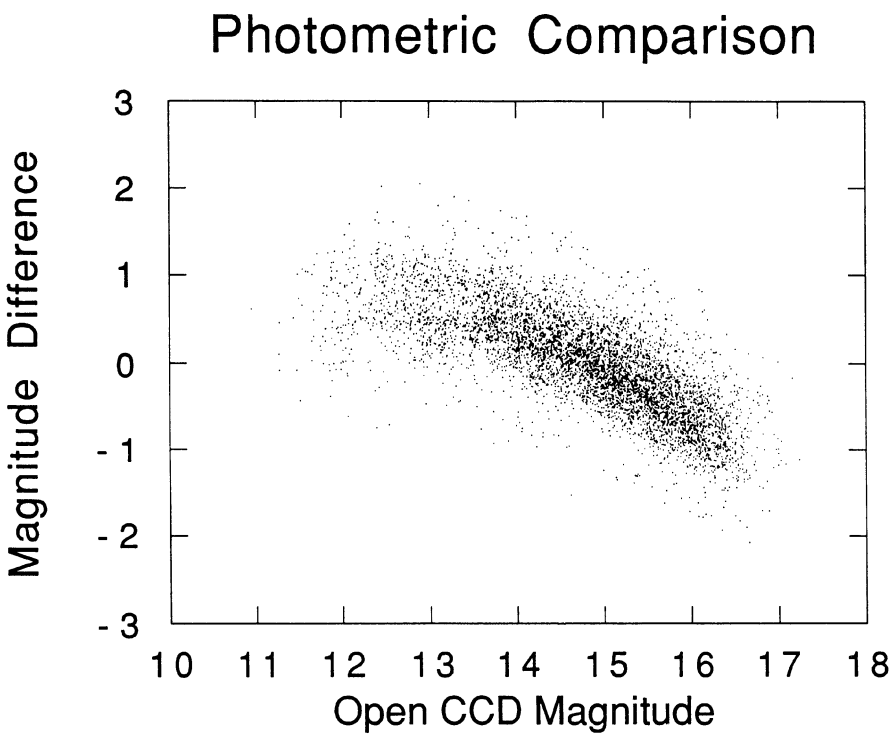

FIG. 2. Photometry. The magnitude difference between photographic V and open CCD magnitudes (in the sense V-CCD) is shown as a function of open CCD magnitude. The apparent discrepancy for the brighter stars is simply due to the different spectral response of the photographic and CCD systems. The photographic magnitudes of the fainter stars are apparently too bright. See text for further discussion.

ture because its amplitude increases with zenith distance and is correlated with the seeing conditions. The amplitude of their position instability is typically half that seen in Fig. 4, as might be expected given the better seeing at the Flagstaff site. However, they also find that the R.A. and Dec. amplitudes are comparable, in contrast to our results.

The apparent precision we have achieved (as described in the previous paragraphs) is nearly good enough to determine whether a given event will be visible on the Earth. However, we feel that systematic effects, to be discussed next, are larger.

4.2 Accuracy

We first assess the astrometric accuracy of the data by comparing the positions of blended Pluto/Charon images, as reduced by our procedures, with the Pluto and Charon ephemerides. Such images appear on two overlapping strips taken 54 min apart that happened to cover Pluto's position at that time. By chance, Charon was near conjunction at that time and the separation between Pluto and Charon perpendicular to the ephemeris was 0.14 arcsec. The center of light of each image was therefore very close to the system's center of mass. Between the observations on the two strips, Pluto had moved about 2.5 arcsec. On both strips, our analysis routinely identified Pluto as a star and tagged it as a potential occultation candidate. On strip 5, the closest approach of Pluto's ephemeris to the Pluto/Charon image was 0.26 arcsec, and the closest approach of Charon's ephemeris was 0.10 arcsec. The closest approach of Pluto's ephemeris to the Pluto/Charon image on strip 6 was 0.36 arcsec, and the closest approach of Charon's ephemeris was 0.22 arcsec. In addition, the time of closest approach was about 10 min earlier than the time the image was exposed. These errors are consistent with the current $\sim$0.5 arcsec estimated error in the DE-130 ephemeris of Pluto (M. Standish, private communication).

The only other check we have for systematic errors is to compare our positions for the stars in MKB's list with their positions for these stars.This is not as complete a check as one would like, since these stars are the same ones used in the plate solution. Nevertheless, it offers some insight into the magnitude of some of the possible systematic errors, notably refraction. Figure 5 shows the results of this comparison. The rms difference between our respective positions is 0.19 arcsec in R.A. and 0.21 arcsec in Dec. Again, the brighter stars show lower differences, but the rms difference seems to approach a larger asymptotic value indicative of systematic effects.

We have computed the expected magnitude of the error introduced by the wavelength dependence of refraction as a function of stellar spectral type. At an altitude of 30°, our worst case, the position difference between an A5 and M5 star is 1.0 arcsec, and between F5 and M5 it is 0.6 arcsec. At a 45° altitude, our best case, the F5-M5 difference is reduced to 0.3 arcsec. Thus, we expect a typical color-dependent position error of the order of 0.3 arcsec. Another systematic effect of importance that does not appear in Fig. 5 is the sys-

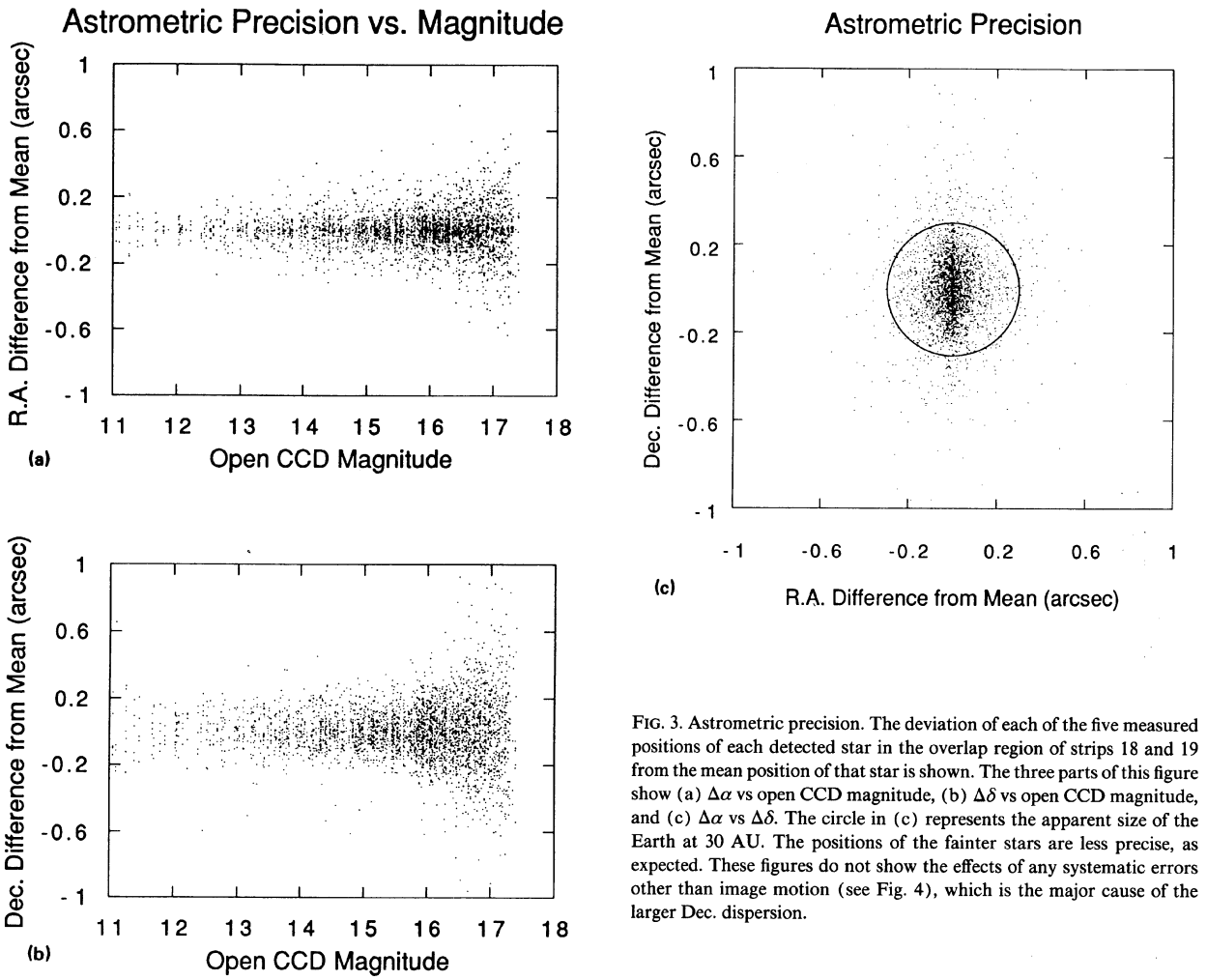

FIG. 3. Astrometric precision. The deviation of each of the five measured positions of each detected star in the overlap region of strips 18 and 19 from the mean position of that star is shown. The three parts of this figure show (a) $\Delta\alpha$ vs open CCD magnitude, (b) $\Delta\delta$ vs open CCD magnitude, and (c) $\Delta\alpha$ vs $\Delta\delta$. The circle in (c) represents the apparent size of the Earth at 30 AU. The positions of the fainter stars are less precise, as expected. These figures do not show the effects of any systematic errors other than image motion (see Fig. 4), which is the major cause of the larger Dec. dispersion.

tematic offset between the coordinate system of the reference stars and Pluto's ephemeris. Based on previous experience, this could also be on the order of 0.3 arcsec, the projected radius of the Earth at Pluto's distance.

5. RESULTS AND DISCUSSION

When comparing the ephemerides of Pluto and Charon with our measured star positions, we included all stars within 1.5 arcsec of the ephemeris as occultation candidates. This rather large impact parameter was chosen so as to include nearly all the stars that will be involved in an occultation that will be observable somewhere on the Earth at the expense of including a number of "false alarms." This value was chosen by considering the following uncertainties: (1) 2σ precision of 0.4 arcsec, (2) possible disagreement between the ephemerides and star coordinate reference system of 0.3 arcsec, (3) typical color-dependent refraction uncertainty of 0.3 arcsec, and (4) uncertainty in the location of the center of mass of the Pluto–Charon system of 0.08 arcsec. In addition to these errors, other factors that increase the impact parameter that must be considered are: one Earth radius of 0.3 arcsec and one Pluto radius of 0.08 arcsec. Some of these factors would add linearly, and some quadratically. In the worst case, they all could add linearly for a total of nearly 1.5 arcsec.

Information concerning the candidate stars and the circumstances of the potential occultations is given in Table 2 for Pluto events and Table 3 for Charon events. The first column in these tables contains a candidate identification number that agrees with the numbers of MKB for those events we have in common, and has "interpolated" decimal values for events falling chronologically between these events. The next three columns include the Universal date and time of closest approach of Pluto or Charon to the star and the geocentric closest approach distance in arcsec. The fifth column gives the position angle in degrees of Pluto or

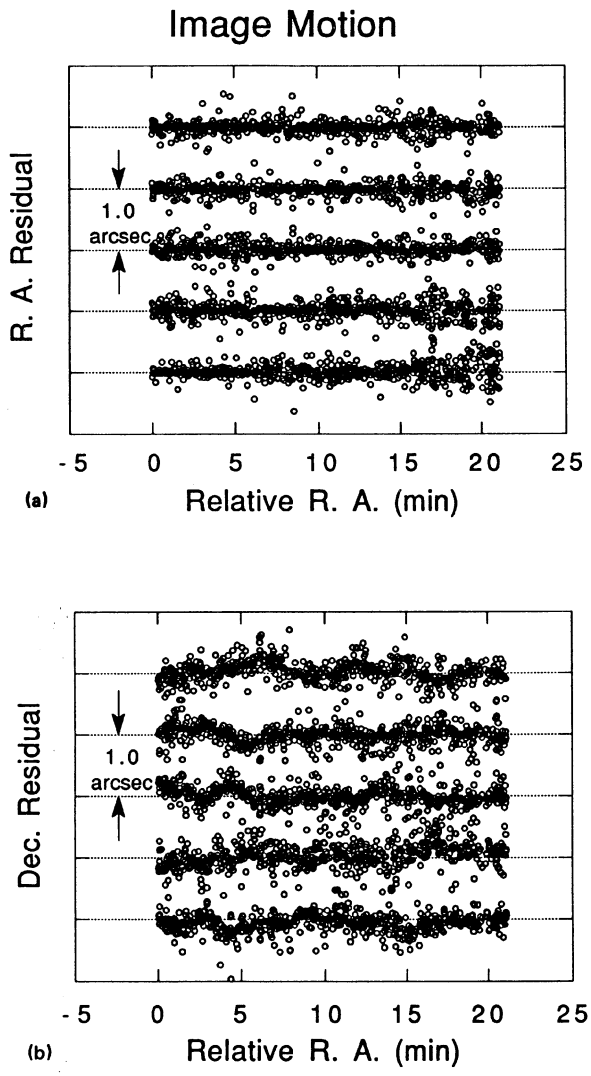

FIG. 4. Image motion. The stars in the overlap region of strips 18 and 19 were observed five times. This figure shows for each of the five strips the deviation of the observed position of each star from the mean of the five positions of that star for R.A. (a) and Dec. (b) as a function of sidereal time in the strip. Each observation has been offset by 1 arcsec for clarity. The dispersion of the individual positions is comparable to the image motion in Dec. The curves in this figure correspond, from bottom to top, to strips 18, 18A, 18B, 19, and 19A. Note that there is much more motion in Dec. than in R.A. See text for further discussion.

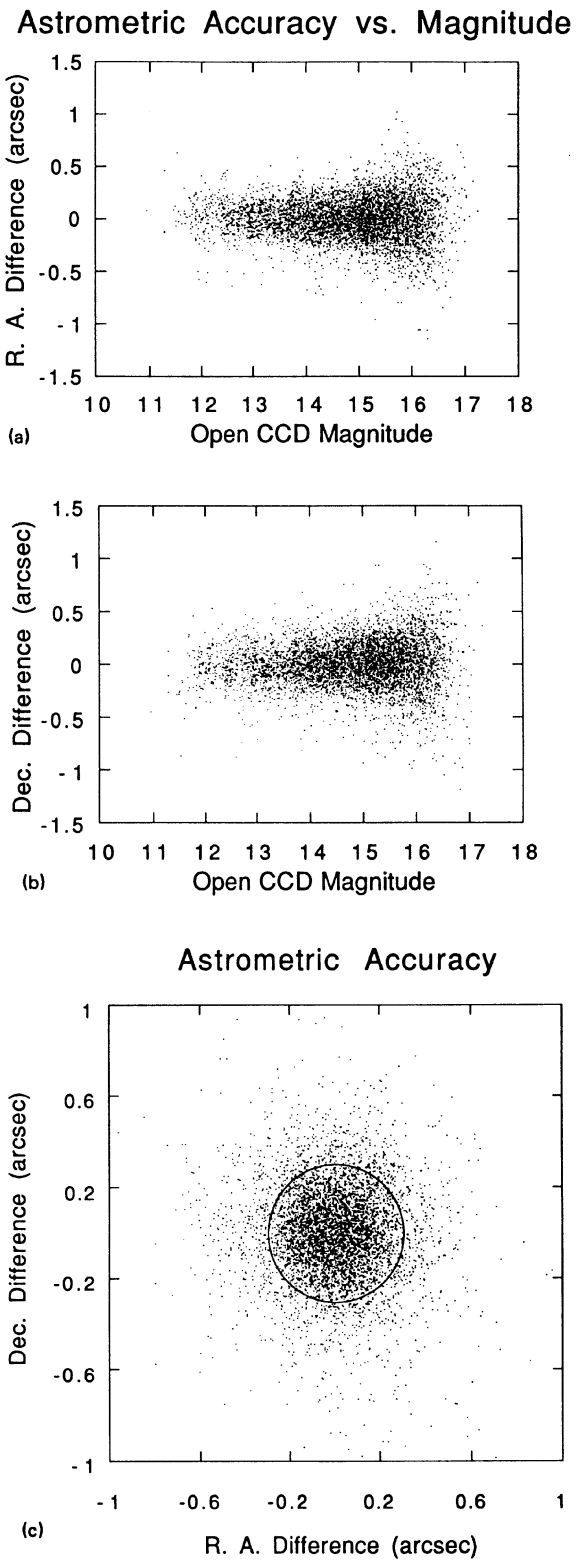

FIG. 5. The deviation of our mean position of each star in the catalog used by MKB from the catalog position of that star is shown. The three parts of this figure show (a) $\Delta\alpha$ vs CCD magnitude, (b) $\Delta\delta$ vs CCD magnitude, and (c) $\Delta\alpha$ vs $\Delta\delta$. The positions of the fainter stars are less precise, as expected. The circle in (c) represents the apparent size of the Earth at 30 AU. These figures show the effects of some, but not all, systematic errors.

Charon relative to the star, measured from north through east, at the time of closest approach. The values tend to cluster near 0°–360° and 180°, corresponding to "s" and "n" in the nomenclature of MKB. Some events occur when the system is moving mostly north–south; these events have position angles near 90° and 270°. The next three columns contain data relating to the quality of the event. The sixth column is the CCD magnitude of the star, the seventh is the velocity of the shadow on the fundamental plane in km/sec, and the eighth is the elongation of the star from the Sun

TABLE 2. Possible occultations by Pluto.

Star ID	---- Closest Approach ----				CCD	sky	Sun	- Star RA -	- Star Dec -	East	Strip Numbers
	-- Date -- y m d	UT h:m	dist (")	PA° (°)	Mag.	vel.	angle	(B1950)	(B1950)	Long	
P10	1990 01 09	23:50	0.38	358	12.9	21.2	63	15:14:25.431	-02:06:07.44	121	10
P10.01	1990 01 10	19:11	0.51	358	17.8	20.8	64	15:14:29.903	-02:06:05.66	-169	10
P10.02	1990 01 23	04:26	1.14	349	17.3	15.5	76	15:15:29.316	-02:04:37.76	39	9,10
P10.04	1990 03 11	15:51	0.99	227	15.8	11.6	122	15:16:13.767	-01:44:36.37	-178	7,8
P10.05	1990 05 29	06:54	0.25	186	16.3	21.6	153	15:09:27.114	-01:06:50.18	-123	2,3
P11	1990 05 31	02:41	0.87	185	16.0	21.3	152	15:09:16.349	-01:06:32.51	-61	2,3
P12	1990 06 20	09:47	0.95	354	14.7	16.5	134	15:07:29.806	-01:06:14.84	171	2,3
P12.01	1990 07 31	23:36	1.16	267	14.9	9.1	96	15:05:52.728	-01:21:42.60	-77	4,5
P12.03	1990 08 29	08:46	1.24	221	15.3	18.5	70	15:06:46.671	-01:42:15.12	117	7
P13	1990 09 05	14:47	0.37	037	14.9	21.4	64	15:07:16.226	-01:48:20.10	19	7,8
P13.01	1990 12 31	10:49	0.04	003	17.3	26.0	52	15:22:23.252	-03:04:19.24	-31	17,18,18A,18B
P13.02	1991 05 09	21:16	0.36	013	18.1	23.5	164	15:20:55.798	-02:14:05.01	43	11
P13.03	1991 05 12	06:06	0.85	012	18.0	23.5	164	15:20:40.803	-02:13:12.75	-91	10,11
P13.04	1991 05 28	12:47	0.76	187	17.9	22.2	156	15:18:58.856	-02:08:42.04	151	10,11
P13.05	1991 06 17	09:52	0.38	177	17.5	18.1	140	15:17:07.464	-02:07:19.16	175	10,11
P13.06	1991 06 22	10:08	0.98	354	16.8	16.7	135	15:16:43.534	-02:07:45.78	166	10,11
P13.07	1991 07 02	09:27	1.08	345	17.4	13.8	126	15:16:02.456	-02:09:31.80	166	10,11
P13.08	1991 08 30	04:06	1.30	042	17.6	17.7	72	15:15:50.917	-02:41:56.90	-170	14,15
P14	1991 09 15	15:07	0.53	212	15.4	24.1	57	15:17:03.735	-02:55:30.68	7	16,17
P14.01	1991 12 29	23:10	0.10	185	16.9	27.5	48	15:31:08.749	-04:02:11.71	146	25,25A,26,26A
P14.02	1992 01 08	21:48	0.77	181	16.2	23.8	57	15:32:15.843	-04:03:08.46	157	25,25A,26,26A
P14.03	1992 01 17	02:20	0.90	177	15.4	20.4	65	15:33:03.648	-04:03:02.34	81	25,25A,26,26A
P15	1992 01 30	12:40	1.55	347	16.8	14.5	78	15:34:05.521	-04:01:15.67	-86	25,25A,26,26A
P15.01	1992 02 05	21:10	0.60	339	17.0	11.8	84	15:34:26.950	-03:59:42.43	140	25,25A,26
P16	1992 03 01	16:25	0.36	258	15.5	7.1	108	15:34:59.048	-03:50:14.60	-172	23,23A,24A
P16.01	1992 03 18	07:35	0.57	040	16.7	12.1	124	15:34:34.736	-03:41:44.84	-56	22,22A,23,23A
P16.02	1992 04 20	04:25	0.17	019	17.2	21.4	154	15:32:17.049	-03:23:57.10	-42	21,21A
P17	1992 05 21	06:17	0.19	009	13.0	23.2	162	15:29:06.360	-03:11:38.98	-101	18,18A,18B,19,19A
P17.01	1992 06 07	01:04	0.36	183	18.0	20.9	150	15:27:23.998	-03:08:43.44	-40	18,19
P17.02	1992 06 11	12:40	1.17	001	17.1	20.0	147	15:26:58.702	-03:08:30.53	140	18,18A,18B,19,19A
P18	1992 09 13	14:28	1.08	213	15.8	22.6	61	15:25:56.842	-03:52:58.55	20	24A,25,25A
P19	1992 09 27	19:43	1.16	027	15.0	27.7	48	15:27:18.119	-04:04:48.19	-71	25,25A,26
P19.01	1993 01 15	22:52	0.77	358	16.9	21.6	62	15:42:03.325	-05:01:02.88	136	33,34
P19.03	1993 01 24	10:44	0.20	174	16.9	17.9	70	15:42:47.701	-05:00:22.39	-49	33,34
P19.04	1993 02 01	11:47	1.10	167	14.6	14.3	78	15:43:21.715	-04:59:01.08	-73	32,33
P19.05	1993 03 18	23:51	0.78	221	17.0	11.3	122	15:43:53.672	-04:41:23.13	61	30,31
P19.06	1993 04 07	21:08	0.86	025	17.7	17.8	141	15:42:45.814	-04:31:00.85	81	29,30
P19.07	1993 04 19	14:47	0.36	199	16.4	20.7	151	15:41:48.020	-04:25:03.79	165	28,29
P19.10	1993 07 11	15:39	0.22	339	17.4	12.3	122	15:34:08.974	-04:13:17.57	68	26,27
P19.11	1993 09 13	19:22	0.11	033	17.4	21.5	63	15:34:57.552	-04:51:09.60	-50	31,32

TABLE 2. (continued)

Star ID	---- Closest Approach ----				CCD	sky	Sun	- Star RA -	- Star Dec -	East	Strip Numbers
	-- Date -- y m d	UT h:m	dist (")	PA° (°)	Mag.	vel.	angle	(B1950)	(B1950)	Long	
P19.12	1993 09 26	23:06	1.03	207	16.9	26.4	51	15:36:09.202	-05:01:39.43	-118	34
P19.13	1993 09 30	21:30	1.18	026	16.8	27.7	47	15:36:33.994	-05:04:51.98	-98	34
P20	1993 10 03	09:14	0.17	205	11.7	28.5	45	15:36:50.514	-05:06:50.88	83	33,34
P20.01	1994 01 01	20:31	0.12	184	17.3	28.0	46	15:49:29.303	-05:57:17.54	-172	40,41
P20.02	1994 02 03	10:58	0.66	348	17.0	14.6	77	15:52:34.644	-05:56:24.29	-60	40,41
P20.03	1994 02 04	21:40	1.43	347	12.0	13.9	78	15:52:40.024	-05:56:07.61	137	40,41
P20.04	1994 04 22	05:48	0.77	018	17.0	20.7	151	15:51:01.753	-05:23:59.20	-60	37
P21	1994 05 15	10:50	1.50	011	14.4	23.4	165	15:48:42.790	-05:14:53.11	-158	35,36
P22	1994 05 18	16:11	1.21	190	15.0	23.5	166	15:48:22.264	-05:13:52.54	117	34,35
P22.01	1994 05 19	13:30	0.88	009	16.3	23.5	165	15:48:16.560	-05:13:39.45	156	34,35
P22.02	1994 06 10	07:25	1.33	002	16.5	21.4	153	15:46:00.840	-05:09:47.19	-133	34,35
P22.03	1994 06 17	08:53	0.25	359	16.8	20.0	147	15:45:20.505	-05:09:33.05	-162	34,35
P22.04	1994 06 27	00:56	0.49	174	16.2	17.5	138	15:44:30.544	-05:10:07.45	-53	34,35
P22.05	1994 07 15	14:03	1.31	157	17.5	12.0	121	15:43:17.248	-05:14:06.92	91	35
P22.07	1994 08 24	04:21	0.64	054	16.9	12.1	85	15:42:52.654	-05:34:00.28	-162	37,38
P22.08	1994 09 18	15:27	1.00	211	17.3	22.2	61	15:44:21.260	-05:52:19.77	6	40
P23	1995 01 05	13:59	0.72	183	16.3	27.6	47	15:58:53.037	-06:53:58.51	-75	48,48A,49,49A
P24	1995 01 08	03:38	0.38	003	13.8	26.7	49	15:59:11.335	-06:54:16.77	77	48,48A,49,49A
P24.01	1995 01 13	22:28	0.43	001	16.6	24.5	55	15:59:50.299	-06:54:40.01	149	48,48A,49,49A
P25.01	1995 04 10	19:42	1.38	023	17.1	17.0	138	16:01:23.955	-06:28:25.55	105	44,45
P25.02	1995 04 21	11:26	1.48	018	16.9	19.8	148	16:00:33.476	-06:23:36.79	-140	44,45
P26	1995 05 07	02:04	0.68	193	15.1	22.6	161	15:59:04.828	-06:17:16.37	-16	43,44
P26.03	1995 06 06	17:14	1.29	184	17.6	22.4	158	15:55:51.216	-06:09:40.89	85	42
P27	1995 06 14	14:37	0.59	181	14.4	21.1	152	15:55:03.778	-06:09:06.21	116	42,43
P28	1995 07 06	03:24	0.05	169	15.2	15.7	133	15:53:13.673	-06:10:47.04	-97	42,43
P28.01	1995 09 22	04:21	0.47	029	16.7	22.5	60	15:53:38.845	-06:51:39.79	171	47,48,48A
P28.02	1995 10 03	17:54	0.34	025	17.1	26.8	50	15:54:45.311	-07:00:15.74	-42	49A
P28.03	1995 10 09	01:46	1.42	023	17.5	28.5	45	15:55:20.402	-07:04:14.59	-165	49A,50
P30	1996 04 17	03:48	0.39	199	15.6	18.2	143	16:10:16.549	-07:23:12.09	-20	51,52
P30.01	1996 04 20	16:54	0.58	018	16.9	19.2	146	16:09:59.243	-07:21:44.16	139	51
P30.02	1996 05 05	20:59	0.98	193	17.7	22.2	159	16:08:35.171	-07:15:52.73	62	51
P30.03	1996 05 08	13:13	1.37	012	15.0	22.6	161	16:08:18.967	-07:15:00.44	176	50,51
P30.04	1996 06 03	12:18	0.24	184	15.7	23.0	162	16:05:34.068	-07:08:41.69	163	50
P30.05	1996 06 15	21:40	0.02	179	16.7	21.3	153	16:04:18.170	-07:07:42.07	11	49,49A,50
P30.06	1996 06 22	14:55	0.74	178	16.5	19.9	147	16:03:40.038	-07:07:45.98	105	49,49A,50
P30.07	1996 06 27	22:21	1.19	355	16.4	18.5	142	16:03:11.999	-07:08:10.51	-11	49,50
P30.08	1996 07 17	23:28	0.62	159	17.0	12.6	124	16:01:47.572	-07:12:06.17	-48	50,51
P30.09	1996 07 23	23:34	0.98	150	16.0	10.7	118	16:01:30.215	-07:14:02.61	-55	50,51
P31	1996 07 28	02:43	0.77	322	15.7	9.5	114	16:01:20.744	-07:15:35.79	-107	50,51
P32	1996 07 28	08:50	1.49	322	16.0	9.5	114	16:01:20.253	-07:15:42.32	160	51
P32.01	1996 08 19	13:54	0.56	251	15.8	9.0	93	16:01:05.682	-07:26:23.61	62	52

TABLE 3. Possible occultations by Charon.

Star ID	---- Closest Approach ----				CCD	sky	Sun	- Star RA -	- Star Dec -	East	Strip Numbers
	-- Date -- y m d	UT h:m	dist (")	PA° (°)	Mag.	vel.	angle	(B1950)	(B1950)	Long	
C10	1990 01 09	23:50	0.96	359	12.9	21.2	63	15:14:25.431	-02:06:07.44	121	10
C10.01	1990 01 10	19:09	0.43	358	17.8	20.9	64	15:14:29.903	-02:06:05.66	-169	10
C10.02	1990 01 23	04:25	1.39	349	17.3	15.5	76	15:15:29.316	-02:04:37.76	39	9,10
C10.03	1990 02 01	08:24	1.00	336	16.0	11.7	85	15:16:01.157	-02:02:22.37	-28	9,10
C10.04	1990 03 11	16:04	1.40	227	15.8	11.8	122	15:16:13.767	-01:44:36.37	178	7,8
C10.05	1990 05 29	06:50	0.60	006	16.3	21.6	153	15:09:27.114	-01:06:50.18	-122	2,3
C11	1990 05 31	02:42	0.75	185	16.0	21.3	152	15:09:16.349	-01:06:32.51	-62	2,3
C12	1990 06 20	09:49	0.17	353	14.7	16.5	134	15:07:29.806	-01:06:14.84	170	2,3
C12.02	1990 08 01	00:09	1.28	267	14.9	9.0	96	15:05:52.728	-01:21:42.60	-85	4,5
C13	1990 09 05	14:36	0.25	217	14.9	21.4	64	15:07:16.226	-01:48:20.10	22	7,8
C13.01	1990 12 31	10:51	0.25	003	17.3	26.0	52	15:22:23.252	-03:04:19.24	-32	17,18,18A,18B
C13.02	1991 05 09	21:12	1.21	013	18.1	23.4	164	15:20:55.798	-02:14:05.01	44	11
C13.03	1991 05 12	06:12	0.08	012	18.0	23.5	164	15:20:40.803	-02:13:12.75	-92	10,11
C13.04	1991 05 28	12:42	0.12	007	17.9	22.2	156	15:18:58.856	-02:08:42.04	152	10,11
C13.05	1991 06 17	09:51	0.40	357	17.5	18.1	140	15:17:07.464	-02:07:19.16	175	10,11
C13.07	1991 07 02	09:26	0.23	345	17.4	13.8	126	15:16:02.456	-02:09:31.80	166	10,11
C13.08	1991 08 30	03:57	0.86	042	17.6	17.5	72	15:15:50.917	-02:41:56.90	-168	14,15
C14	1991 09 15	15:08	0.33	212	15.4	24.2	57	15:17:03.735	-02:55:30.68	7	16,17
C14.01	1991 12 29	23:12	0.35	184	16.9	27.5	48	15:31:08.749	-04:02:11.71	146	25,25A,26,26A
C14.02	1992 01 08	21:45	0.84	181	16.2	23.8	57	15:32:15.843	-04:03:08.46	158	25,25A,26,26A
C15	1992 01 30	12:43	1.05	346	16.8	14.5	78	15:34:05.521	-04:01:15.67	-86	25,25A,26,26A
C15.01	1992 02 05	21:18	0.10	338	17.0	11.8	84	15:34:26.950	-03:59:42.43	138	25,25A,26
C16	1992 03 01	17:10	0.43	258	15.5	7.2	108	15:34:59.048	-03:50:14.60	175	23,23A,24A
C16.01	1992 03 18	07:24	1.06	040	16.7	12.0	124	15:34:34.736	-03:41:44.84	-54	22,22A,23,23A
C16.02	1992 04 20	04:29	0.09	019	17.2	21.3	154	15:32:17.049	-03:23:57.10	-43	21,21A
C17	1992 05 21	06:16	0.78	009	13.0	23.1	162	15:29:06.360	-03:11:38.98	-101	18,18A,18B,19,19A
C17.01	1992 06 07	01:01	0.26	183	18.0	20.9	150	15:27:23.998	-03:08:43.44	-39	18,19
C17.02	1992 06 11	12:44	0.27	000	17.1	20.0	147	15:26:58.702	-03:08:30.53	140	18,18A,18B,19,19A
C18	1992 09 13	14:29	0.80	213	15.8	22.7	61	15:25:56.842	-03:52:58.55	20	24A,25,25A
C19	1992 09 27	19:36	0.55	027	15.0	27.7	48	15:27:18.119	-04:04:48.19	-69	25,25A,26
C19.01	1993 01 15	22:53	0.35	358	16.9	21.5	62	15:42:03.325	-05:01:02.88	136	33,34
C19.02	1993 01 18	02:34	1.33	177	17.3	20.7	64	15:42:15.347	-05:00:54.52	78	34
C19.03	1993 01 24	10:45	0.68	354	16.9	17.9	70	15:42:47.701	-05:00:22.39	-50	33,34
C19.04	1993 02 01	11:42	1.20	168	14.6	14.3	78	15:43:21.715	-04:59:01.08	-71	32,33
C19.05	1993 03 19	00:11	1.15	221	17.0	11.2	122	15:43:53.672	-04:41:23.13	56	30,31
C19.06	1993 04 07	21:18	0.07	025	17.7	17.8	141	15:42:45.814	-04:31:00.85	79	29,30
C19.07	1993 04 19	14:54	0.71	199	16.4	20.7	151	15:41:48.020	-04:25:03.79	163	28,29
C19.08	1993 05 03	23:02	1.34	015	15.9	23.0	162	15:40:24.916	-04:18:38.98	27	27,27A,28,28X
C19.09	1993 06 23	05:22	1.03	355	16.8	17.8	139	15:35:23.756	-04:09:40.90	-118	26,26A,27
C19.10	1993 07 11	15:40	0.28	158	17.4	12.4	122	15:34:08.974	-04:13:17.57	68	26,27

TABLE 3. (continued)

Star ID	---- Closest Approach ----				CCD	sky	Sun	- Star RA -	- Star Dec -	East	Strip Numbers
	-- Date -- y m d	UT h:m	dist (")	PA° (°)	Mag.	vel.	angle	(B1950)	(B1950)	Long	
C19.11	1993 09 13	19:13	0.30	213	17.4	21.6	63	15:34:57.552	-04:51:09.60	-47	31,32
C20	1993 10 03	09:07	0.83	205	11.7	28.5	45	15:36:50.514	-05:06:50.88	84	33,34
C20.01	1994 01 01	20:31	0.80	184	17.3	27.9	46	15:49:29.303	-05:57:17.54	-172	40,41
C20.02	1994 02 03	11:04	0.52	347	17.0	14.6	77	15:52:34.644	-05:56:24.29	-61	40,41
C20.04	1994 04 22	05:40	1.37	018	17.0	20.7	151	15:51:01.753	-05:23:59.20	-57	37
C20.05	1994 05 04	14:47	1.15	194	13.5	22.7	161	15:49:50.462	-05:18:40.61	152	35,36
C20.06	1994 05 05	21:19	1.23	194	17.1	22.8	161	15:49:42.714	-05:18:10.54	53	35
C21	1994 05 15	10:55	0.62	011	14.4	23.5	165	15:48:42.790	-05:14:53.11	-160	35,36
C22	1994 05 18	16:08	0.33	190	15.0	23.4	166	15:48:22.264	-05:13:52.54	118	34,35
C22.01	1994 05 19	13:31	1.33	009	16.3	23.4	165	15:48:16.560	-05:13:39.45	156	34,35
C22.02	1994 06 10	07:26	0.51	002	16.5	21.5	153	15:46:00.840	-05:09:47.19	-133	34,35
C22.03	1994 06 17	08:51	0.13	179	16.8	20.0	147	15:45:20.505	-05:09:33.05	-162	34,35
C22.04	1994 06 27	00:59	0.19	173	16.2	17.5	138	15:44:30.544	-05:10:07.45	-54	34,35
C22.05	1994 07 15	14:10	0.62	156	17.5	12.0	121	15:43:17.248	-05:14:06.92	89	35
C22.06	1994 07 21	07:55	0.92	147	16.5	10.3	116	15:43:01.816	-05:16:05.72	177	35,36
C22.07	1994 08 24	04:11	0.69	054	16.9	12.3	85	15:42:52.654	-05:34:00.28	-159	37,38
C22.08	1994 09 18	15:22	1.03	211	17.3	22.4	61	15:44:21.260	-05:52:19.77	7	40
C23	1995 01 05	13:54	1.18	184	16.3	27.6	47	15:58:53.037	-06:53:58.51	-74	48,48A,49,49A
C24	1995 01 08	03:41	0.34	002	13.8	26.7	49	15:59:11.335	-06:54:16.77	76	48,48A,49,49A
C24.01	1995 01 13	22:30	0.07	181	16.6	24.4	55	15:59:50.299	-06:54:40.01	148	48,48A,49,49A
C25.01	1995 04 10	19:48	1.46	022	17.1	16.8	138	16:01:23.955	-06:28:25.55	104	44,45
C26	1995 05 07	02:11	1.21	193	15.1	22.6	161	15:59:04.828	-06:17:16.37	-18	43,44
C26.01	1995 05 11	00:23	1.46	192	12.6	23.0	163	15:58:40.625	-06:15:52.28	4	43,44
C26.02	1995 05 17	16:16	0.78	190	17.1	23.3	166	15:57:58.604	-06:13:47.41	120	42,43
C26.03	1995 06 06	17:15	0.79	183	17.6	22.3	158	15:55:51.216	-06:09:40.89	84	42
C27	1995 06 14	14:42	1.31	181	14.4	21.1	152	15:55:03.778	-06:09:06.21	115	42,43
C28	1995 07 06	03:19	0.08	350	15.2	15.7	133	15:53:13.673	-06:10:47.04	-95	42,43
C28.01	1995 09 22	04:31	1.16	029	16.7	22.5	60	15:53:38.845	-06:51:39.79	169	47,48,48A
C28.02	1995 10 03	17:59	0.45	024	17.1	26.7	50	15:54:45.311	-07:00:15.74	-43	49A
C28.03	1995 10 09	01:44	0.84	023	17.5	28.4	45	15:55:20.402	-07:04:14.59	-164	49A,50
C30	1996 04 17	03:55	1.19	199	15.6	18.3	143	16:10:16.549	-07:23:12.09	-22	51,52
C30.01	1996 04 20	16:51	1.29	018	16.9	19.1	146	16:09:59.243	-07:21:44.16	139	51
C30.04	1996 06 03	12:14	0.62	005	15.7	22.9	162	16:05:34.068	-07:08:41.69	165	50
C30.05	1996 06 15	21:35	0.73	001	16.7	21.2	153	16:04:18.170	-07:07:42.07	12	49,49A,50
C30.06	1996 06 22	14:51	0.14	358	16.5	19.8	147	16:03:40.038	-07:07:45.98	106	49,49A,50
C30.07	1996 06 27	22:15	1.42	356	16.4	18.6	142	16:03:11.999	-07:08:10.51	-9	49,50
C30.08	1996 07 17	23:29	0.24	340	17.0	12.5	124	16:01:47.572	-07:12:06.17	-48	50,51
C30.09	1996 07 23	23:34	0.29	151	16.0	10.6	118	16:01:30.215	-07:14:02.61	-55	50,51
C31	1996 07 28	02:27	0.04	143	15.7	9.6	114	16:01:20.744	-07:15:35.79	-103	50,51
C32	1996 07 28	08:32	0.76	322	16.0	9.5	114	16:01:20.253	-07:15:42.32	165	51
C32.01	1996 08 19	14:29	0.38	250	15.8	9.0	93	16:01:05.682	-07:26:23.61	54	52

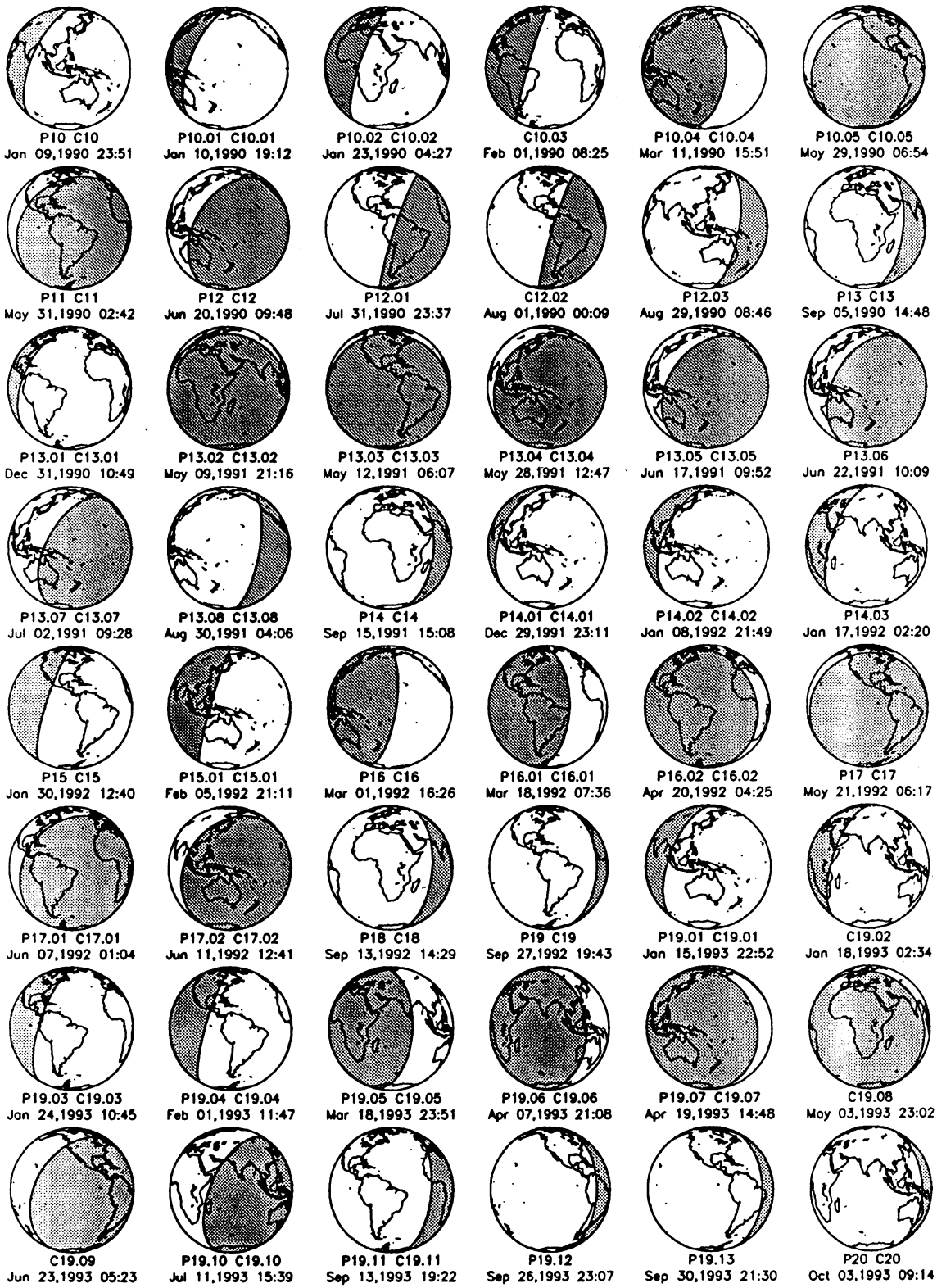

FIG. 6. Each frame in this figure shows the Earth as seen from the direction of Pluto at the approximate time of the occultation of the indicated star by Pluto or Charon. The shaded region is that part of the Earth where the Sun is more than 12° below the horizon. The sub-Pluto point is in the center of each globe.

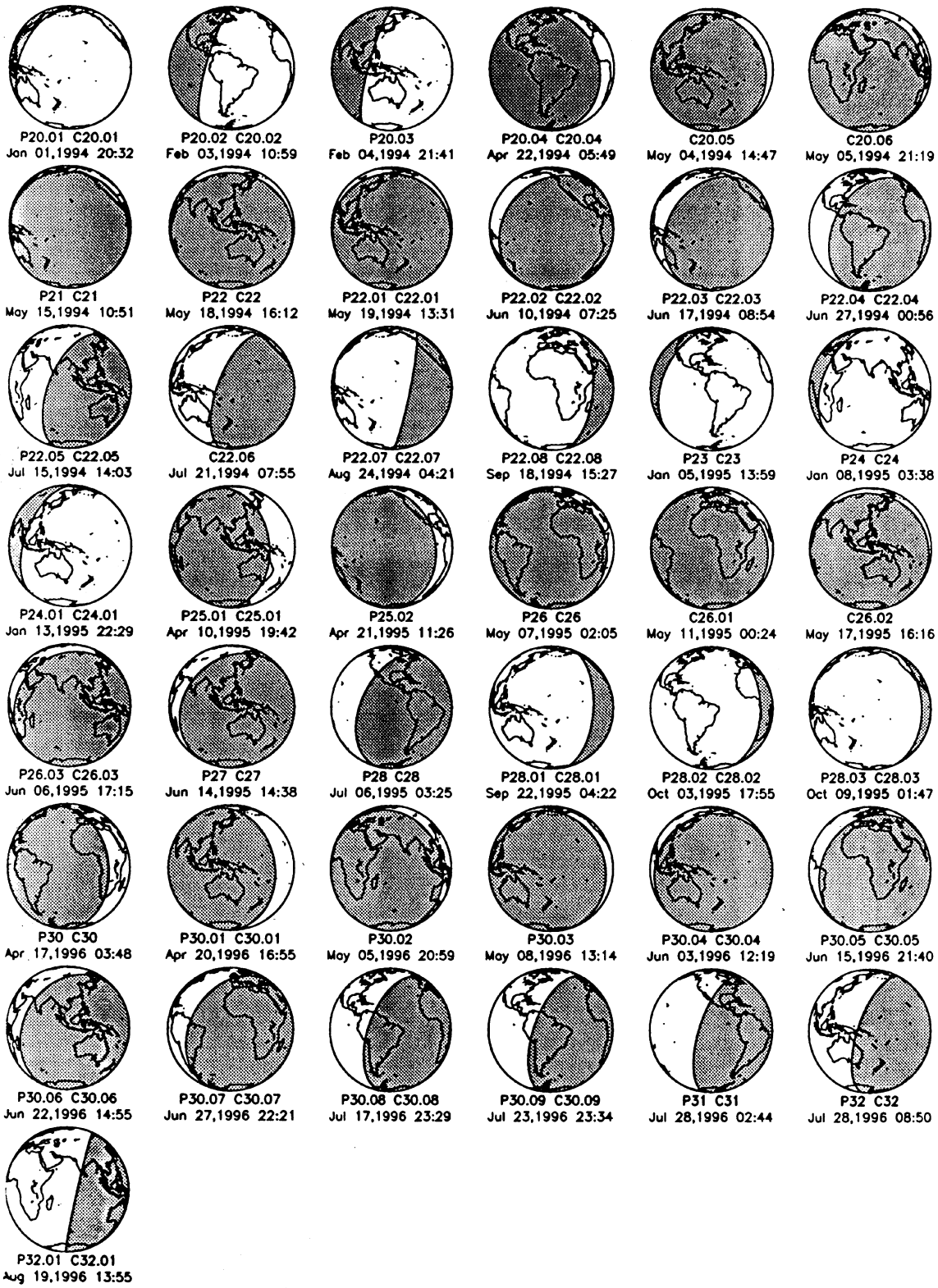

FIG. 6. (continued)

measured in degrees. The next two columns are the B1950.0 coordinates of the star. Note that the declination is essentially the sub-Pluto latitude on the Earth for that event. This, taken with the next column, the sub-Pluto east longitude in degrees, helps define the area of observability on the Earth. Figure 6 shows the region of observability for each star. The last column lists the strips on which each candidate star appeared. This is useful for comparing with Table 1 to see what the observing conditions were for each strip the candidate appears on.

The event velocity (column 7) is included to allow the S/N ratio of the event to be estimated by means of Fig. 7. Generally it is best to use as short an integration time as is practical, unless one must pay a noise penalty. Maximum integration times for a Pluto event with a velocity v km/s would be $20/v$ s to obtain three data points per scale height, high in the atmosphere. This is the minimum sampling required to obtain a reliable value for the scale height of an isothermal atmosphere (French *et al.* 1978). The integration times should be shorter to properly characterize the "kink" in the lightcurve. For Charon events, the integration times should be significantly shorter than $40/v$ s if one is to resolve the issue of a possible Charon atmosphere (Elliot & Young 1991). Since the major source of noise throughout the range of Fig. 7 is shot noise from the occulted star and the Pluto–Charon system, the S/N ratio for a given spatial resolution will be proportional to $1/\sqrt{v}$.

To aid in identification of these rather faint candidate stars, we have provided finder charts in Fig. 8. Each finder chart is taken directly from our flattened CCD strip scans, scaled as needed to allow the faint stars to appear clearly.

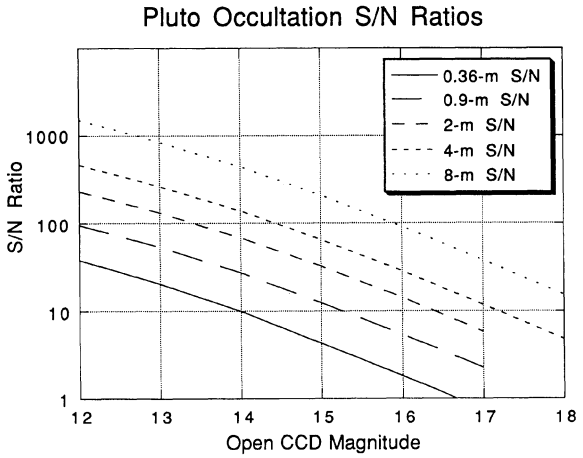

FIG. 7. S/N ratio vs open CCD magnitude. The curves in this figure show the expected S/N ratio of an occultation observation using a CCD camera at 1 s time resolution. The curves correspond, from top to bottom, to observations using an 8, 4, 2, 0.9, or 0.36 m telescope. (The Kuiper Airborne Observatory has a 0.9 m telescope; the commonly used 14 in. Schmidt–Cassegrain portable telescopes are 0.36 m.) The event velocity was assumed to be 20 km/s and the combined R magnitude of Pluto and Charon was assumed to be 14. The CCD response was approximated as having a central wavelength of 0.65 μm, a bandwidth of 0.4 μm, a quantum efficiency of 40% and 10 electron read noise. It was further assumed that 80% of the light fell within 9 CCD pixels, each 1 arcsec square.

The events found include all the events of MKB except P25, and about twice as many additional events. The P25 image was reexamined by Arnold Klemola, who found it to be stellar in appearance, but who also found that the star did not appear on the Palomar Observatory Sky Survey. We also found an unusually large difference between our declination and MKB's for the star P15. We found this star to be about 0.7 mag fainter than the typical limit for MKB's stars. Arnold Klemola kindly reexamined the image of this star on the original plate as well and found it to be a very weak image. We believe that our position for P15 is the more reliable of the two.

The brightest stars in our list are those involved in the events P10/C10, P17/C17, P20/C20, P20.03, C20.05, P24/C24, and C26.01. Those events with a sky plane velocity less than 10 km/s are P12.01, C12.02, P16/C16, P31/C31, P32/C32, and P32.01/C32.01. A number of events have nearly the same miss distance for both Pluto and Charon, indicating that it is likely that either both events will be observable or that neither one will be. These events are of particular interest because they would provide a much more precise value for the semimajor axis of Charon's orbit if they were well observed. The stars that are occulted when the apparent separation between Pluto and Charon is less than 0.2 arcsec are: 10.01, 11, 14.02, 16, 16.02, 17.01, 19.04, 20.02, 22.07, 22.08, 24, 25.01, 28, 28.02, and 32.01.

The fact that we have used a new method allowing observation of fainter stars than conventional photographic searches implies that the conventional means for refining the astrometry and producing a prediction may need improvement. Benedict *et al.* (1991) find that they can achieve a positional precision of 0.04 arcsec for 17th magnitude stars with their CCD/Transit Instrument, a strip-scanning CCD camera using a V filter with 1.55 arcsec pixels mounted on a 1.8 m telescope on Kitt Peak pointing close to the zenith. This indicates that a method similar to that presented in this paper—practiced at a better site and with a telescope of longer focal length—would be sufficiently accurate to provide the needed improvement. Alternatively, astrometry with *Hubble Space Telescope* images may provide the needed refinement in the event predictions.

6. CONCLUSIONS

We have carried out a search for stars that will be occulted by Pluto or Charon over the period 1990–1995, and including much of 1996. The search was made using a CCD camera in a scanning mode, and reached a magnitude limit of approximately $R = 17.5$. The S/N ratio for a 1 s integration of these events would be greater than 20 for the Keck telescope, and greater than 8 for a 4 m telescope. This signal-to-noise would be more than adequate to accomplish some of our goals, such as identifying substantial changes in Pluto's atmospheric structure as its heliocentric distance changes, and perhaps resolving the haze-layer issue. All the events identified by MKB for this period were found with the exception of P25, which also does not appear on the Palomar Sky Survey. About twice as many additional candidate events were found. The astrometric accuracy is sufficient to make a "short list" of promising candidates, but further astrometry will be required to identify the events that actually will be observable and to refine the predictions.

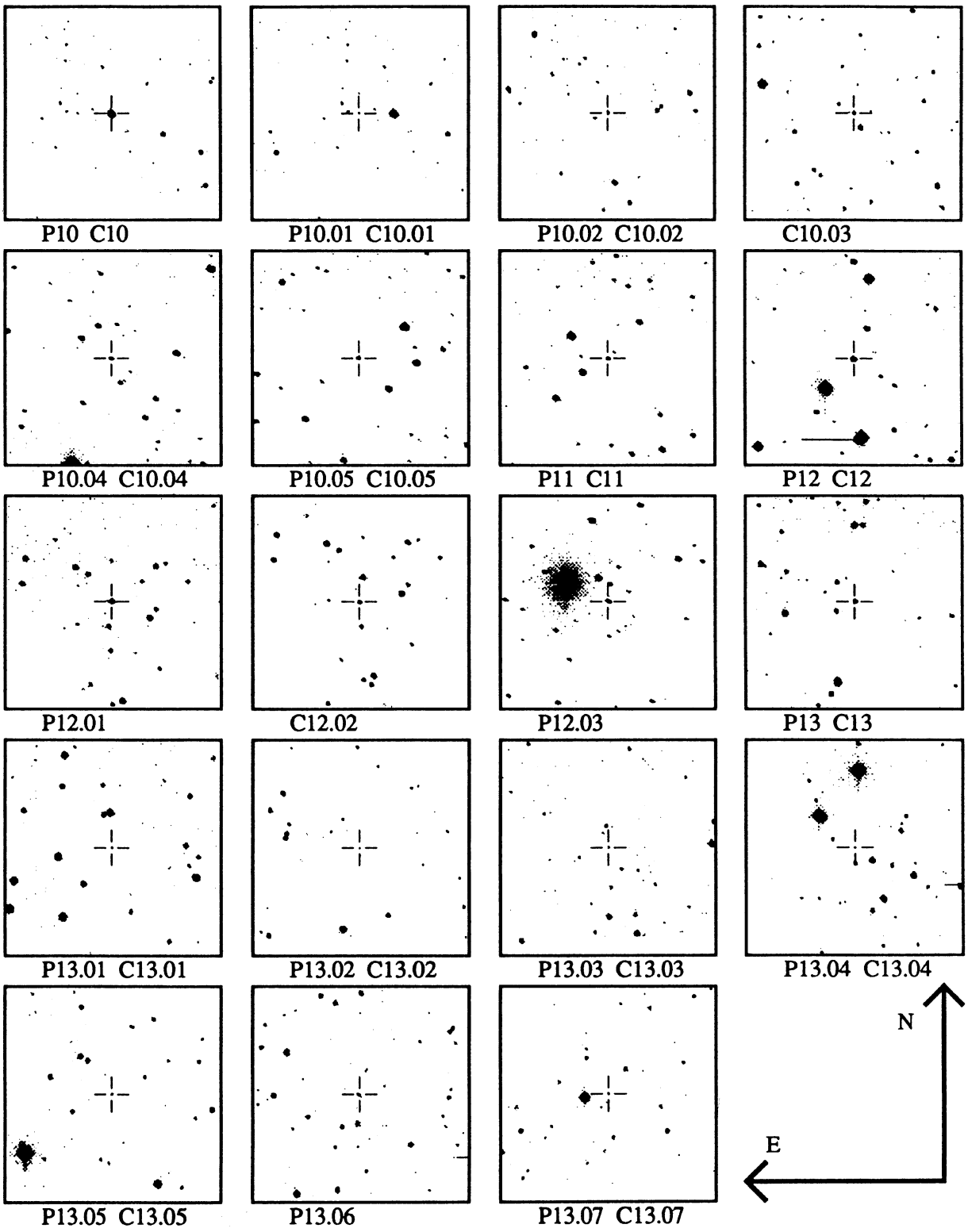

FIG. 8. Finder charts. These finder charts were derived directly from our strip scan images. The boxes are each 6.88 arcmin on a side, and the occulted star is marked. Each chart is labeled with event identifications corresponding to those in Tables 2 and 3.

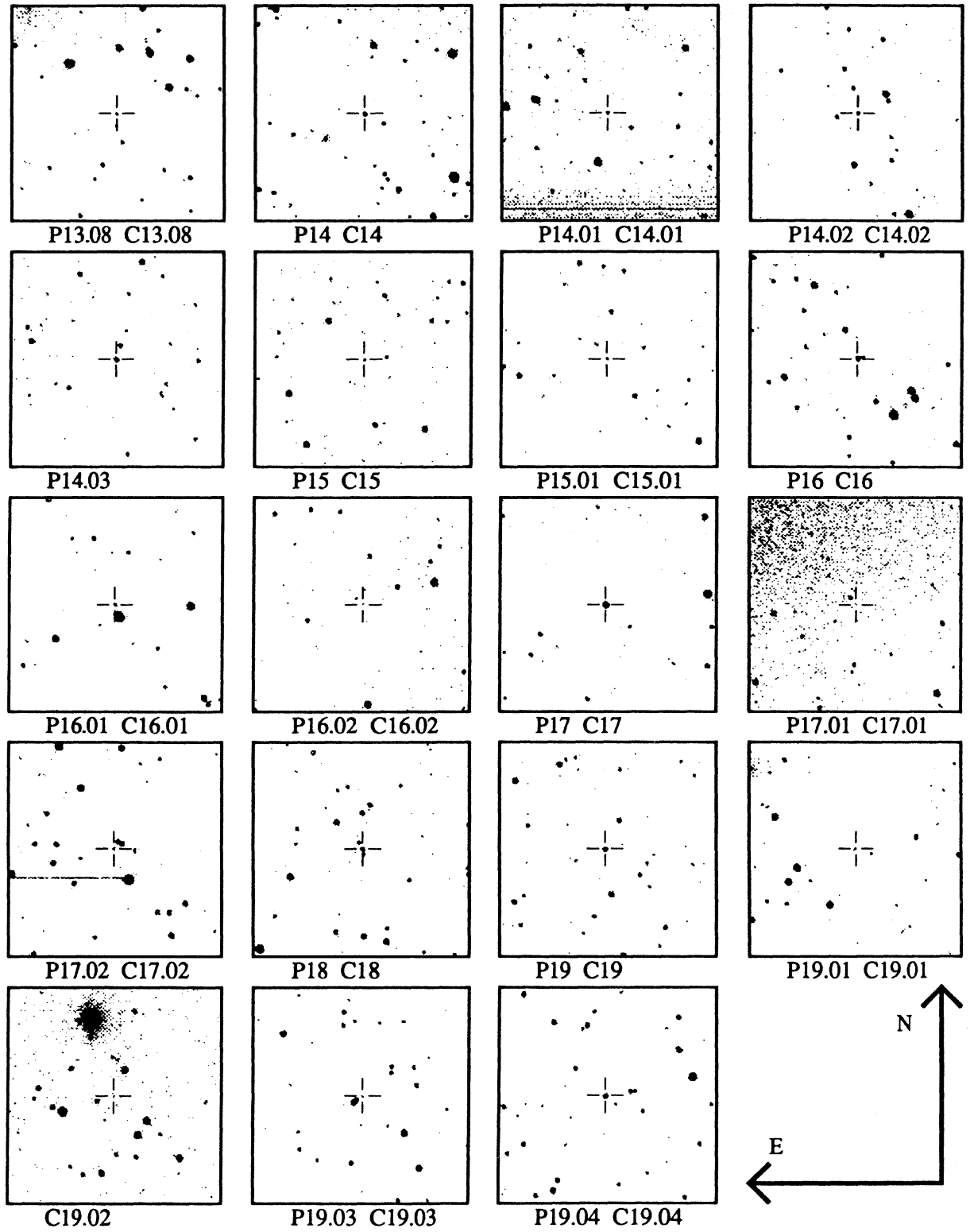

FIG. 8. (continued)

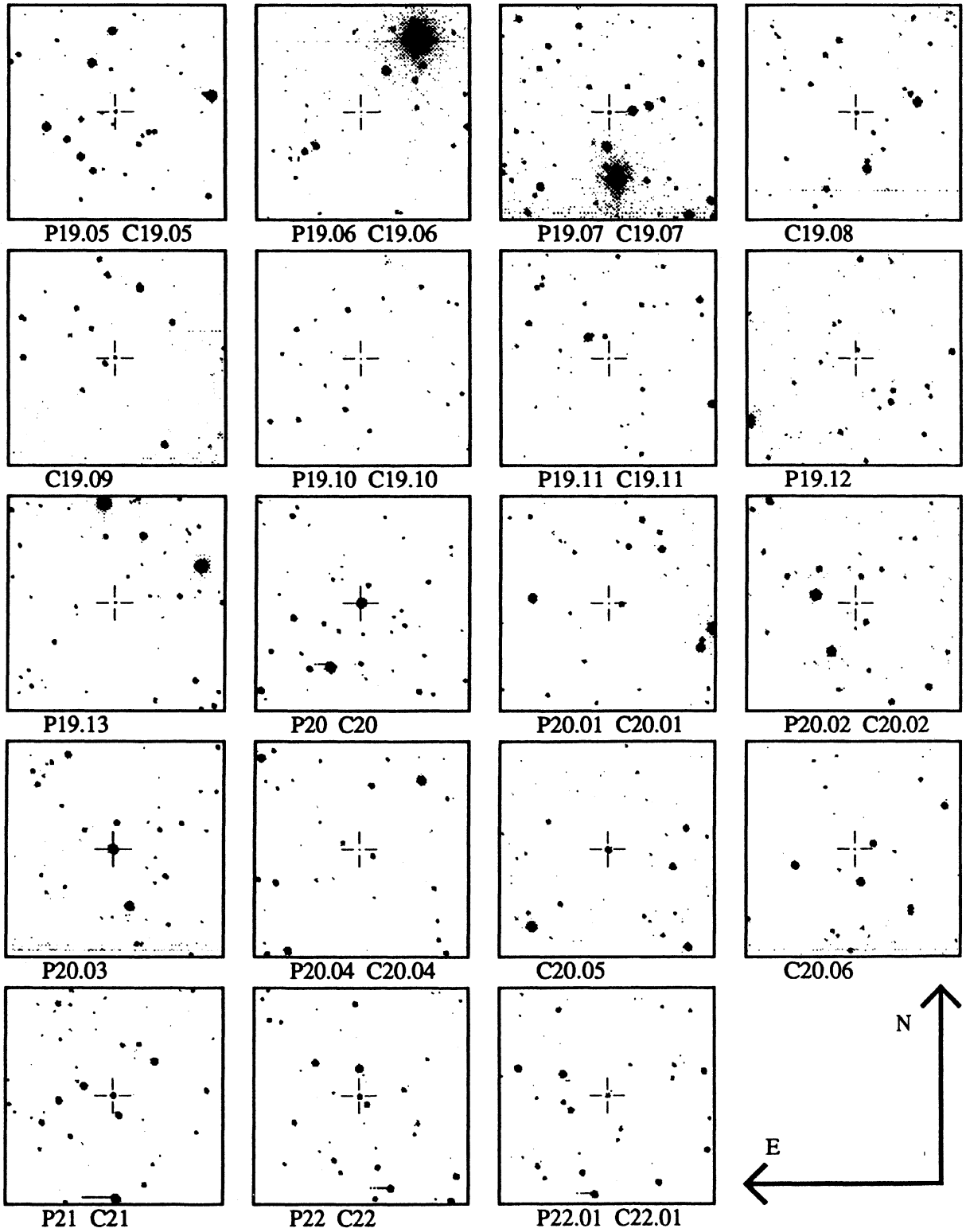

FIG. 8. (continued)

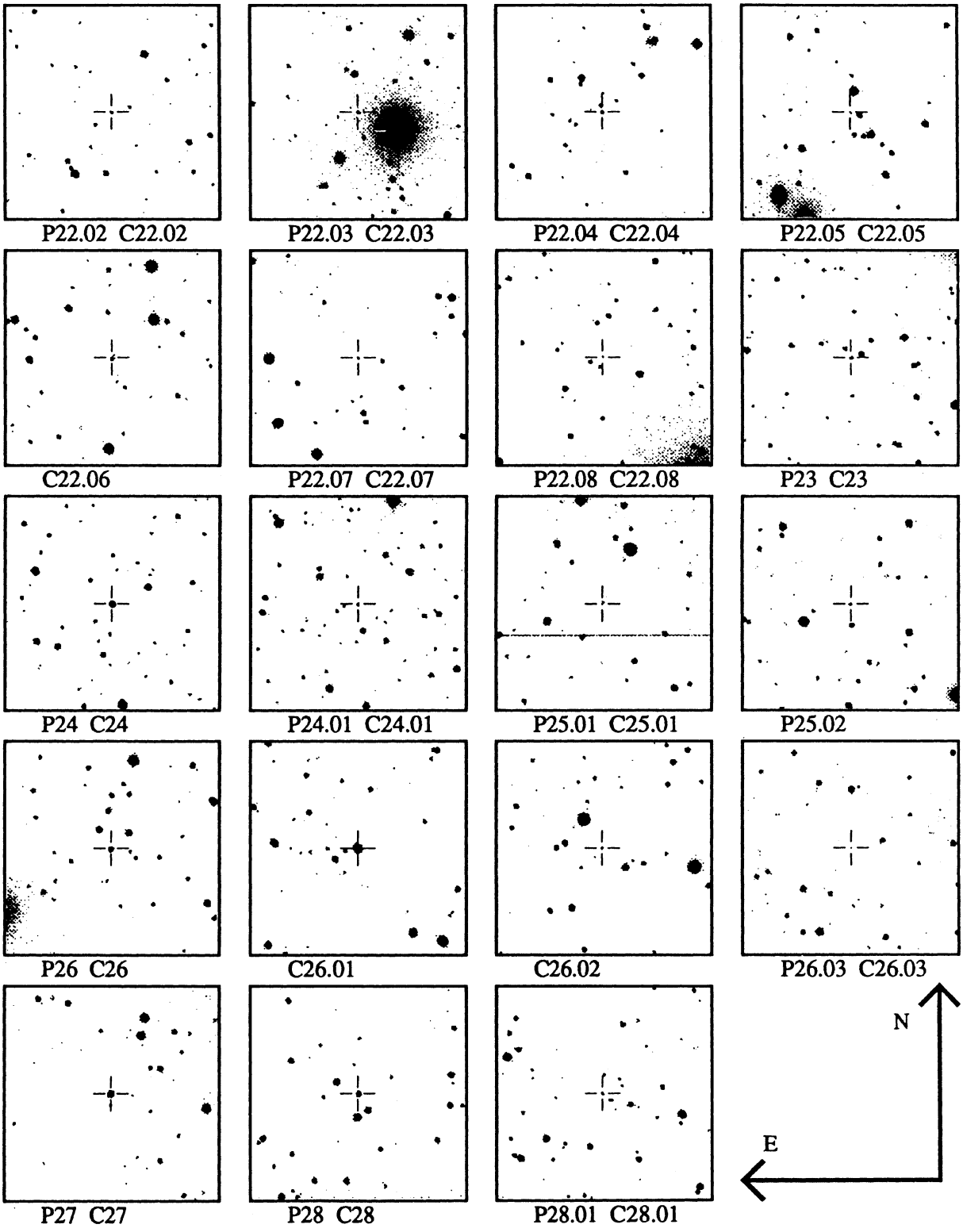

FIG. 8. (continued)

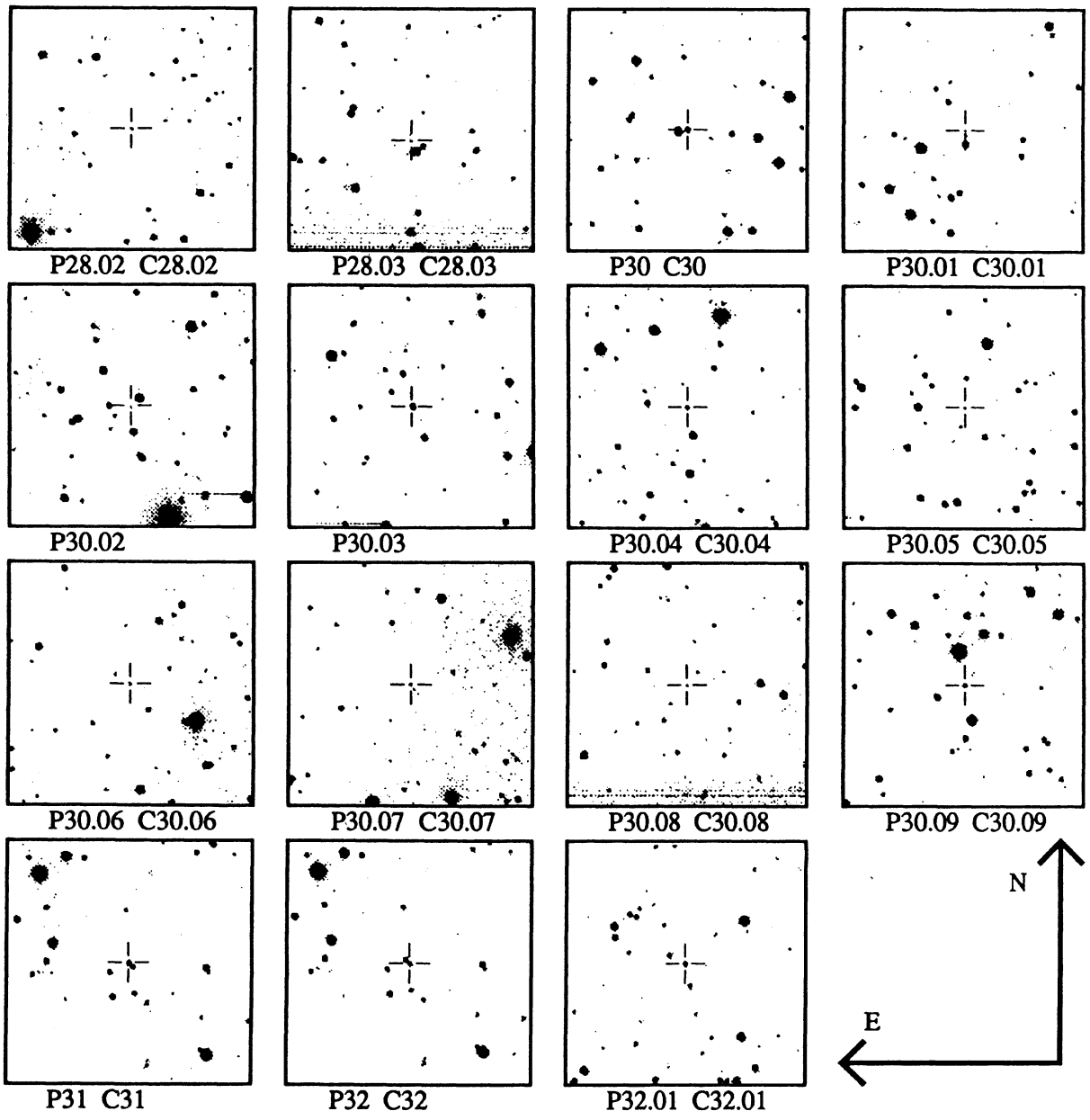

FIG. 8. (continued)

We would like to give our heartfelt thanks to R. Meserole for his work in getting the camera and observatory ready for the observing run. A. Bosh, J. Harrington, M. Holman, and L. Young made many of the observations used in this work. L. Young wrote the program which performed plate registration for the strips. We would like to give special thanks to the IRAF staff at NOAO for providing us with the beta test version of DAOPHOT. It worked well for us! Figure 1 was made using the STARCHART program, written by C. Counterman. L. Wasserman produced Fig. 6 for us, greatly improving the usefulness of the occultation candidate list. We thank R. Stone and M. Standish for useful discussions. Finally, we thank D. Mink and A. Klemola for their invaluable help in carrying out this work, providing us our reference star catalog and ephemerides, and for numerous useful discussions.

REFERENCES

Aldering, G. 1990, Ph.D. dissertation, University of Michigan, Chap. 2
Benedict, G. F., McGraw, J. T., Hess, T. R., Cawson, M. G. M., and Keane, M. J. 1991, AJ, 101, 279
Binzel, R. P., Tholen, D. J., Tedesco, E. F., Buratti, B. J., and Nelson, R. M. 1985, Sci, 228, 1193
Binzel, R. P. 1989, Geophys. Res. Lett., 16, 1205
Bosh, A. S., Elliot, J. L., Kruse, S. E., Baron, R. L., Dunham, E. W., and French, L. M. 1986, Icarus, 66, 556
Dunham, E. W., Baron, R. L., Elliot, J. L., Vallerga, J. V., Doty, J. P., and Ricker, G. R. 1985, PASP, 97, 1196
Elliot, J. L., Dunham, E. W., Bosh, A. S., Slivan, S. M., Young, L. A., Wasserman, L. H., and Millis, R. L. 1989, Icarus, 77, 148
Elliot, J. L., and Young, L. A. 1991, Icarus, 89, 244
French, R. G., Elliot, J. L., and Gierasch, P. J. 1978, Icarus, 33, 186
Gehrels, T., Marsden, B. G., McMillan, R. S., and Scotti, J. V. 1986, AJ, 91, 1242
Luppino, G. A. 1989, PASP, 101, 931
Mink, D. J., Klemola, A. R., and Buie, M. W. 1991, AJ, 101, 2255
Standish, E. M. 1987, Jet Propulsion Laboratory Interoffice Memorandum IOM 314.6-891
Stetson, Peter B. 1987, AJ, 99, 191
Stier, M. T. 1986, SPIE, 619, 120
Tholen, D. J., and Buie, M. W. 1989, BAAS, 21, 981
Tody, D. 1986, SPIE, 627, 733
Walker, A. R. 1980, MNRAS, 192, 47p
Williams, B. 1988, senior thesis in physics, MIT